Available online at www.synsint.com

Synthesis and Sintering

ISSN 2564-0186 (Print), **ISSN** 2564-0194 (Online)

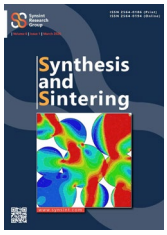

Research article

Explainable AI for predicting crystallinity in doped hydroxyapatite: Implications for biomedical applications

Shahla Azizi *

Department of Electrical and Electronic Engineering, Eastern Mediterranean University, Gazimağusa, Mersin 10, Türkiye

A B S T R A C T

Hydroxyapatite (HAp) is a widely used bioactive material in medical applications such as bone tissue engineering, where the crystallinity plays a critical role in determining mechanical strength, bioactivity, and bioelectric behavior. The crystallinity is strongly affected by complex interactions between dopant elements and processing conditions. In this study, a public database was used to develop an explainable artificial intelligence (AI) framework to predict the crystallinity of multi-doped HAp based on compositional parameters. A public dataset comprising 37 samples with various dopants (e.g., Sr, Zn, Ag, F, and transition metals), processing temperatures, and duration was used. Three machine learning (ML) models, including XGBoost, random forest, and decision tree, were developed using all features. An explainable AI method, Shapley additive explanations (SHAP), was used to identify the most relevant features for each model. The features relevant to all models were selected (temperature, processing duration, Zn, HAp, Er, and Al). Model performance was assessed before and after feature reduction. XGBoost achieved the best performance with all features (R^2 = 0.917, root mean squared error as RMSE = 6.03), while feature reduction slightly decreased its performance (R^2 = 0.881, RMSE = 6.18). In contrast, RF and DT showed notable improvements after feature selection, with RF increasing from R^2 = 0.814 to 0.872 and DT from R^2 = 0.574 to 0.688, indicating reduced overfitting and improved generalization. Final model interpretation using SHAP revealed that processing parameters (time and temperature) dominate crystallinity prediction, followed by specific dopants such as Zn and Er. It was demonstrated that combining SHAP-based consensus feature selection with ML provides both accurate prediction and meaningful interpretation, offering valuable insights into the factors governing HAp crystallinity.

KEYWORDS

Sintering
XGBoost
XAI
Random forest

OPEN ACCESS

1. Introduction

Hydroxyapatite (HAp), a calcium phosphate bioceramic, is one of the most widely used biomaterials in bone tissue engineering as it has compositional similarity to the inorganic phase of natural bone and excellent biocompatibility, biodegradability, thermal stability, osteoconductivity, and bioactivity [1, 2]. Owing to this structural similarity, HAp is extensively used as an implant material for repairing and regenerating damaged skeletal tissues [2]. With the increasing demand for biomedical applications, including rehabilitation and aesthetic treatments, numerous synthesis techniques for HAp nanoparticles have been developed [2, 3].

HAp can be found in natural sources such as animals, plants, and minerals like Limestone [4]. However, synthesized HAp can be produced using chemical methods such as solid-state reactions, the sol-gel process, and emulsion, with synthesis and processing conditions

* Corresponding author. *E-mail address:* shahla.alikamar@emu.edu.tr (S. Azizi)

Received 22 July 2025; Received in revised form 27 March 2026; Accepted 27 March 2026.

https://doi.org/10.53063/synsint.2026.61229

affecting their morphology, structure, and physicochemical properties [4,5]. Among the modification strategies, ion doping has emerged as an effective approach to tailor the structural and functional properties of HAp. Incorporation of foreign ions can alter key characteristics such as lattice structure, porosity, and crystallinity [6]. Among these properties, crystallinity plays an important role in determining mechanical strength, dissolution rate, bioactivity, and bioelectric behavior [7].

The literature showed that various metals can be used for doping. For instance, Fe-doped HAp exhibited increased durability, bioactivity, and proliferation [6]. Metal doping could significantly enhance the antimicrobial performance of HAp, with ions such as silver (Ag), copper (Cu), zinc (Zn), and strontium (Sn) exhibiting measurable inhibition zones against pathogens like Escherichia coli (E. coli) and Staphylococcus aureus (S. aureus), whereas pure HAp shows negligible activity [8]. In addition, manganese (Mn)-doped HAp has been shown to possess a biomimetic structure closely resembling natural bone apatite, along with high cytocompatibility, indicating strong potential for bone tissue engineering applications [9]. Despite these advancements, the specific effects of different dopant ions on HAp crystallinity remain insufficiently explored.

Recently, machine learning (ML) and deep learning (DL) approaches have emerged as powerful tools for predicting material properties, including crystallinity, bioactivity, and biocompatibility, before experimental synthesis. Studies have shown that models such as XGBoost can accurately predict the crystallinity of ion-doped HAp, with Mg^{2+} and Zn^{2+} identified as key factors influencing crystallinity [7]. Furthermore, crystallinity has been identified as the dominant parameter affecting photocatalytic performance, with extreme learning machine (ELM) models achieving high prediction accuracy [10]. Advanced approaches, including graph convolutional neural networks combined with explainable artificial intelligence (XAI), have also demonstrated strong capability in capturing structure–property relationships in HAp using multiscale datasets, achieving near density functional theory (DFT) accuracy [11].

In this study, we aim to predict the crystallinity of ion-doped HAp using ML models combined with XAI techniques. XGBoost, random forest (RF), and decision tree (DT) models are employed, while Shapley additive explanations (SHAP) are used to interpret the influence of different dopants on crystallinity.

2. Methods

All analyses were performed in Python 3.12, using scikit-learn, XGBoost, SHAP, pandas, NumPy, and matplotlib libraries. Computations were performed on a standard workstation with 16 GB RAM and an Intel i7 CPU.

2.1. Dataset preparation

The public dataset that was used in this study is available at https://github.com/Fajar2006/HAP [7]. It contains information about ion concentrations (%) including HAp (%), strontium (Sr), Zn, Ag, fluorine (F), nickel (Ni), Cu, Iron (Fe), erbium (Er), boron (B), aluminum (Al), barium (Ba), tungsten (W), molybdenum (Mo), magnesium (Mg), sintering temperature (°C), time (hours) and crystallinity (%). This database was collected from previously published literature [7]. There were 105 samples; rows with missing temperature, time, or crystallinity were removed to ensure dataset integrity. The final dataset contained 37 samples with 17 quantitative features. All features were numeric. Non-numeric columns (e.g., reference URLs) were excluded prior to modeling.

2.2. Machine learning models

Three supervised ML models, including XGBoost, RF, and DT, were used to predict crystallinity. All models were implemented using default scikit-learn compatible interfaces and evaluated under identical experimental conditions.

Extreme gradient boosting (XGBoost)

XGBoost is an ensemble learning method based on gradient boosting of decision trees. It builds models sequentially, where each new tree minimizes the residual errors of the previous ones. It employs level-wise tree growth, sparsity-aware splits, and approximate histogram-based splits for scalability [12]. In this study, these parameters were used: Number of boosting rounds (trees) = 300, maximum depth of each tree = 4, step size shrinkage = 0.05, fraction of samples used for each tree = 0.8, fraction of features used per tree = 0.8.

Random forest (RF)

RF builds an ensemble of decorrelated DTs via bagging, where each DT is trained on bootstrapped data subsets and random feature subsets at splits. Predictions aggregate via majority vote (classification) or averaging (regression), reducing variance and improving generalization [13]. The parameters were 200 trees in the forest and the default setting for other parameters. This model is effective for handling nonlinear relationships and noisy data.

Decision tree (DT)

DT recursively partitions data based on feature thresholds to minimize impurity measures like entropy. Each internal node represents a decision, leaves denote class predictions, and splits are chosen greedily for optimal local gain [14]. DTs are interpretable but prone to overfitting, often addressed via pruning. A maximum depth of 5 was used to avoid overfitting.

2.3. Model evaluation

The models' performance metrics, including coefficient of determination (R^2), adjusted R^2, root mean squared error (RMSE), and mean absolute error (MAE), were evaluated. R^2 and adjusted R^2 measure the proportion of variance explained by the model, RMSE evaluates prediction error magnitude, and MAE measures average absolute prediction deviation [15].

2.4. Explainable AI (XAI) and feature selection (SHAP-based consensus)

To interpret model predictions and define the best features, an explainable AI method, SHAP, was used. Based on cooperative game theory, SHAP assigns each feature a contribution value, representing its influence on the crystallinity relative to a baseline prediction. Positive SHAP values indicate that a feature increases the predicted crystallinity, whereas negative values indicate a decreasing effect. In this study, TreeExplainer was employed for the models to efficiently compute accurate feature contribution values, leveraging the inherent structure of these models. Global feature importance was obtained by averaging the absolute SHAP values across all samples. To ensure robustness, a multi-model consensus strategy was employed: SHAP-based feature rankings were computed independently for each model, and features were ranked based on their frequency of appearance in the top-10 most important features. Features appearing in all models' top-

10 rankings were selected as the final feature subset. This consensus-based approach reduces model-specific bias and improves the stability of selected predictors.

2.5. Final model training and interpretation

After feature selection, the final predictive models were retrained using only the selected features. The same leave-one-out cross-validation (LOOCV) framework was applied to evaluate model performance before and after dimensionality reduction.

The best-performing model (XGBoost) was further analyzed using SHAP summary bar plots to investigate the relationship between key predictors and crystallinity. These visualizations provided information about the magnitude and direction of feature effects.

3. Results

Fig. 1 represents the SHAP bar plots showing the importance of the first 10 features for each model. As these figures show, processing time, and temperature, HAp, Zn, Er, and Al are the parameters that are relevant in all models. Hence, they were used to train XGBoost, RF, and DT using LOOCV method.

Table 1 shows the evaluation metrics for these ML models before and after feature reduction. The evaluation of ML models revealed that XGBoost significantly outperformed the other algorithms in predicting HAp crystallinity. Overall, the XGBoost model demonstrated the highest predictive accuracy when trained on the full feature set, achieving an R^2 of 0.917 and an RMSE of 6.03. The RF model showed moderate performance (R^2 = 0.81), while the DT model exhibited the lowest accuracy (R^2 = 0.57), indicating limited generalization capability when using all available features. After applying SHAP-based consensus feature reduction, the performance trends changed notably. The XGBoost model experienced a slight decrease in predictive performance (R^2 = 0.88, RMSE = 6.18), suggesting that the removed features contained some useful predictive information. On the contrary, both RF and DT models showed clear improvements. The RF model improved from R^2 = 0.81 to 0.87 and reduced its RMSE from 10.08 to 7.97, indicating enhanced generalization and reduced variance. Similarly, the DT model improved from R^2 = 0.57 to 0.68, with RMSE decreasing from 13.17 to 11.70, demonstrating that feature reduction mitigated overfitting.

These results indicate that feature selection had a model-dependent effect. While XGBoost, which is inherently robust to irrelevant features due to its boosting mechanism, performed best with the full feature set, simpler models such as RF and DT benefited significantly from dimensionality reduction.

Fig. 2a presents the parity plot for the XGBoost model trained on the selected features. The predictions show strong relationships with experimental crystallinity values, with most data points distributed close to the diagonal line, indicating good predictive accuracy. A few deviations are observed, particularly at lower crystallinity values, suggesting slightly reduced model performance in that range. Overall, the distribution confirms the robustness of the model after feature reduction.

Fig. 2b illustrates the SHAP summary plot for the selected features, characterizing their contributions to the model predictions. Among the features, processing time and temperature exhibit the largest impact, with higher values generally contributing positively to crystallinity.

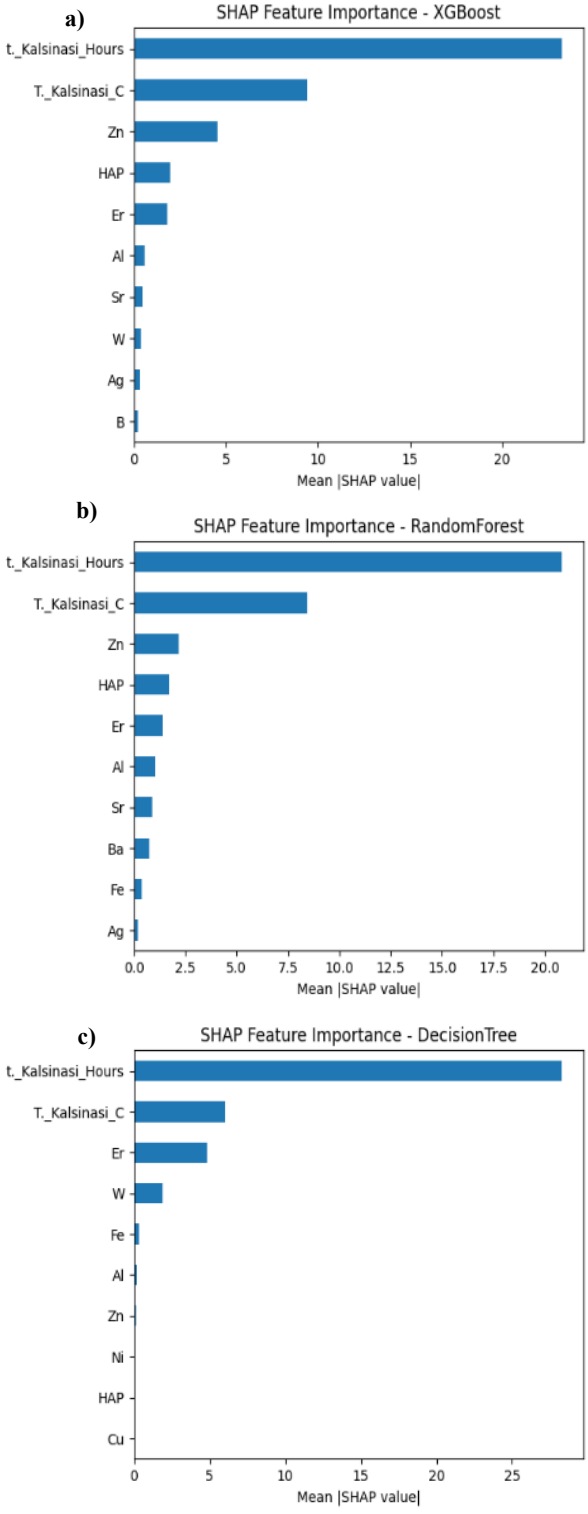

Fig. 1. SHAP bar plots for all models. a) XGBoost, b) random forest, and c) decision tree.

This indicates that processing conditions are the dominant factors influencing the output.

Dopant-related features such as Zn, HAp, Er, and Al show comparatively small but still meaningful contributions. Zn and HAp

Table 1. Performance of machine learning methods before and after feature reduction.

	Basic model				Models trained with reduced features			
	R^2	Adjusted R^2	RMSE	MAE	R^2	Adjusted R^2	RMSE	MAE
XGBoost	0.917	0.85	6.03	6.03	0.88	0.86	6.18	6.18
Random forest	0.81	0.68	10.08	10.08	0.87	0.85	7.97	7.97
Decision tree	0.57	0.27	13.17	13.17	0.68	0.63	11.7	11.7

display both positive and negative effects depending on their values, suggesting nonlinear interactions with crystallinity. On the contrary, Al exhibits a relatively limited influence, with SHAP values clustered closer to zero.

4. Discussions

The present study demonstrates that ML models, particularly XGBoost, can effectively capture the complex, nonlinear relationships among dopant composition, processing parameters (time and temperature), and HAp crystallinity. The higher performance of XGBoost ($R^2 \approx 0.88$–0.92) shows its suitability for modeling small and heterogeneous datasets, where intricate feature interactions and nonlinear dependencies are prevalent. Compared to conventional models, its boosting-based architecture enables robust learning even in the presence of limited data and potential noise.

The SHAP-based analysis further enhances the interpretability of the model by defining the underlying structure–property relationships. Processing time and temperature were identified as the most influential variables governing crystallinity, which is consistent with their well-established thermodynamic and kinetic roles in sintering processes. These parameters directly influence grain growth, phase stability, and the degree of crystal ordering, thereby dominating the crystallization behavior of HAp. Higher temperature and prolonged duration likely enhance atomic diffusion, reduce lattice defects, and promote crystal maturation, thereby increasing crystallinity [16–19]. These results are in line with the previous research showing that XGBoost had the highest performance in predicting crystallinity, and time and temperature were the most contributing parameters [7].

Among dopants, Zn, Er, and Al consistently showed positive contributions across models. This suggests that these ions may act as structural stabilizers or promote lattice ordering within the HAp matrix. Zn is known to influence osteogenic activity and can substitute into Ca sites, potentially enhancing crystal growth [5]. The consistent importance of Er is notable and may indicate an underexplored role in lattice distortion control or crystallite refinement. It was shown that Er dopant leads to thermal stability in HAp [20]. The role of Zn in crystallinity is in line with previous findings [7]. Al doping reduces the crystallinity of HAp, producing smaller, more disordered nanocrystals and increasing lattice defects [21]. At low–moderate Al levels is accompanied by a slight increase in thermal stability but overall lower structural regularity and solubility of the HAp phase [22].

The lower performance of the DT model highlights two inherent characteristics of the dataset: the presence of complex nonlinear interactions among features, and the limited sample size. As a single-tree model, DT is prone to high variance and overfitting, particularly in small datasets where slight variations in training data can lead to substantially different tree structures. This instability reduces its generalization capability, as reflected in its lower predictive accuracy. The RF shows improved performance relative to DT due to its

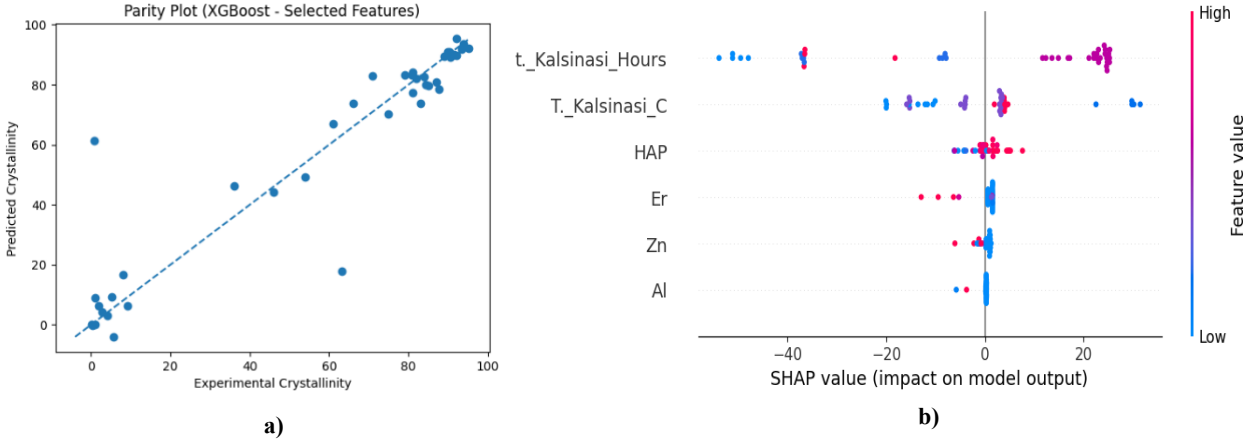

Fig. 2. a) Parity plot comparing experimental and predicted crystallinity values obtained using the XGBoost model with selected features and b) SHAP summary plot illustrating the relative importance and directional impact of the selected features on crystallinity prediction.

ensemble-based variance reduction; however, its performance was lower than XGBoost. This suggests that, although bagging mitigates overfitting to some extent, it may still struggle to fully capture intricate feature interactions under data-scarce conditions. In contrast, the higher performance of XGBoost indicates that boosting-based approaches are more effective in handling low-sample, high-dimensional materials datasets, as they iteratively refine residual errors and better model complex nonlinear dependencies.

Clinical implications

Although this study is computational, the findings have direct implications for biomedical and clinical materials design. Crystallinity is strongly correlated with mechanical strength, degradation rate, and biological stability of HAp-based implants. The identification of key predictors (temperature, time, Zn, Er, and Al) provides a data-driven pathway for optimizing implant fabrication protocols.

Dopant-informed control of crystallinity can be used to engineer scaffolds with tailored resorption rates and osteoconductivity, improving outcomes in bone defect repair and orthopedic reconstruction. The ML framework enables rapid screening of dopant combinations without exhaustive experimental synthesis, reducing cost and time in preclinical biomaterials development. With further data expansion, such models could support patient-specific implant design, where crystallinity and degradation rates are tuned according to metabolic and anatomical requirements.

Limitations

Despite promising results, several limitations should be acknowledged. The final dataset included only 37 samples, which significantly limits model generalizability and increases the risk of overfitting, even with cross-validation. The dataset is compiled from multiple studies with potentially inconsistent experimental protocols, measurement techniques, and reporting standards, introducing hidden bias and noise.

Only compositional and processing parameters were included. Other relevant factors, such as pH, pressure, precursor type, and synthesis route, were not consistently available. Although SHAP improves interpretability, feature attribution does not confirm causal relationships; it only reflects learned statistical associations.

5. Conclusions

Our results show the effectiveness of ML for predicting HAp crystallinity from dopant composition and processing conditions. Among the evaluated models, XGBoost achieved the highest predictive accuracy and stability, highlighting its suitability for complex, small-scale materials datasets.

XAI analysis revealed that sintering temperature and time are the dominant drivers of crystallinity, while Zn, Sr, Al and Er are the most influential dopants. These findings provide both predictive capability and interpretable views into material design.

Overall, our finding offers a powerful data-driven approach for guiding the optimization of HAp-based biomaterials and may contribute to more efficient development of high-performance bone substitute materials.

CRediT authorship contribution statement

Shahla Azizi: Conceptualization, Methodology, Resources, Writing – original draft, Writing – review & editing.

Data availability

The data underlying this is available at https://github.com/Fajar2006/HAP.

Declaration of competing interest

The authors declare no competing interests.

Funding and acknowledgment

The author would like to thank the Department of Electrical and Electronics Engineering at Eastern Mediterranean University for providing an enriching environment and valuable resources that significantly contributed to the completion of this paper. The author is grateful for access to extensive library resources, advanced laboratories, and collaborative spaces that fostered an environment conducive to academic exploration and innovation.

Declaration of Generative AI and AI-assisted technologies in the writing process

During the preparation of this work, the author used ChatGPT to edit and improve the writing style. After using this tool/service, the author reviewed and edited the content as needed and takes full responsibility for the content of the publication.

References

[1] E. Fiume, G. Magnaterra, A. Rahdar, E. Verné, F. Baino, Hydroxyapatite for biomedical applications: A short overview, Ceramics. 4 (2021) 542–563. https://doi.org/10.3390/ceramics4040039.

[2] R.O. Kareem, N. Bulut, O. Kaygili, Hydroxyapatite biomaterials: a comprehensive review of their properties, structures, medical applications, and fabrication methods, J. Chem. Rev. 6 (2024) 1–26. https://doi.org/10.48309/jcr.2024.415051.1253.

[3] Y. Jin, G. Lou, J. Zhao, F. Du, M. Jin, et al., Hydroxyapatite in medical aesthetics: Current status, advantages, and limitations, Chinese Chem. Lett. (2026) 112513. https://doi.org/10.1016/j.cclet.2026.112513.

[4] V.G. DileepKumar, M.S. Sridhar, P. Aramwit, V.K. Krut'ko, O.N. Musskaya, et al., A review on the synthesis and properties of hydroxyapatite for biomedical applications, J. Biomater. Sci. Polym. Ed. 33 (2022) 229–261. https://doi.org/10.1080/09205063.2021.1980985.

[5] M.S.F. Hussin, H.Z. Abdullah, M.I. Idris, M.A.A. Wahap, Extraction of natural hydroxyapatite for biomedical applications—A review, Heliyon. 8 (2022) e10356. https://doi.org/10.1016/j.heliyon.2022.e10356.

[6] S. Balakrishnan, V.P. Padmanabhan, R. Kulandaivelu, T.S.S.N. Nellaiappan, S. Sagadevan, et al., Influence of iron doping towards the physicochemical and biological characteristics of hydroxyapatite, Ceram. Int. 47 (2021) 5061–5070. https://doi.org/10.1016/j.ceramint.2020.10.084.

[7] A.F. Pradana, I.S. Sari, A. Federico, R.S.P. Kaban, Y. Yusuf, et al., The prediction of hydroxyapatite crystallinity under various ion doping using machine learning, Results Chem. 18 (2025) 102701. https://doi.org/10.1016/j.rechem.2025.102701.

[8] M.L. Habib, S.A. Disha, M.S. Hossain, M.N. Uddin, S. Ahmed, Enhancement of antimicrobial properties by metals doping in nano-crystalline hydroxyapatite for efficient biomedical applications,

Heliyon. 10 (2024) e23845. https://doi.org/10.1016/j.heliyon.2023.e23845.
[9] S. Lala, M. Ghosh, P.K. Das, T. Kar, S.K. Pradhan, Mechanical preparation of nanocrystalline biocompatible single-phase Mn-doped A-type carbonated hydroxyapatite (A-cHAp): effect of Mn doping on microstructure, Dalt. Trans. 44 (2015) 20087–20097. https://doi.org/10.1039/C5DT03398E.
[10] W. Liu, Y. Fang, H. Qiu, C. Bi, X. Huang, et al., Determinants and performance prediction on photocatalytic properties of hydroxyapatite by machine learning, Opt. Mater. 146 (2023) 114510. https://doi.org/10.1016/j.optmat.2023.114510.
[11] Z. Liu, Y. Shi, H. Chen, T. Qin, X. Zhou, et al., Machine learning on properties of multiscale multisource hydroxyapatite nanoparticles datasets with different morphologies and sizes, NPJ Comput. Mater. 7 (2021) 142. https://doi.org/10.1038/s41524-021-00618-1.
[12] T. Sugihartono, B. Wijaya, M. Marini, A.P. Alkayess, H.A. Anugerah, Optimizing stunting detection through SMOTE and machine learning: a comparative study of XGBoost, random forest, SVM, and k-NN, J. Appl. Data Sci. 6 (2025) 667–682. https://doi.org/10.47738/jads.v6i1.494.
[13] L. Breiman, Random forests, Mach. Learn. 45 (2001) 5–32. https://doi.org/10.1023/A:1010933404324.
[14] V.G. Costa, C.E. Pedreira, Recent advances in decision trees: An updated survey, Artif. Intell. Rev. 56 (2023) 4765–4800. https://doi.org/10.1007/s10462-022-10275-5.
[15] M.M. Mundu, J.I. Sempewo, A. Goparaju, D.E. Uti, Comparative analysis of model evaluation metrics in energy systems, environmental modeling, and sustainability science, Int. J. Energy Res. 2026 (2026) 6170467. https://doi.org/10.1155/er/6170467.
[16] G. Muralithran, S. Ramesh, The effects of sintering temperature on the properties of hydroxyapatite, Ceram. Int. 26 (2000) 221–230. https://doi.org/10.1016/S0272-8842(99)00046-2.
[17] S. Aarthy, D. Thenmuhil, G. Dharunya, P. Manohar, Exploring the effect of sintering temperature on naturally derived hydroxyapatite for bio-medical applications, J. Mater. Sci. Mater. Med. 30 (2019) 21. https://doi.org/10.1007/s10856-019-6219-9.
[18] J. Vivanco, J. Slane, R. Nay, A. Simpson, H.-L. Ploeg, The effect of sintering temperature on the microstructure and mechanical properties of a bioceramic bone scaffold, J. Mech. Behav. Biomed. Mater. 4 (2011) 2150–2160. https://doi.org/10.1016/j.jmbbm.2011.07.015.
[19] M. Trzaskowska, V. Vivcharenko, A. Przekora, The impact of hydroxyapatite sintering temperature on its microstructural, mechanical, and biological properties, Int. J. Mol. Sci. 24 (2023) 5083. https://doi.org/10.3390/ijms24065083.
[20] B.K. Mahmood, O. Kaygili, N. Bulut, S.V Dorozhkin, T. Ates, et al., Effects of strontium-erbium co-doping on the structural properties of hydroxyapatite: An Experimental and theoretical study, Ceram. Int. 46 (2020) 16354–16363. https://doi.org/10.1016/j.ceramint.2020.03.194.
[21] M. Wang, L. Wang, C. Shi, T. Sun, Y. Zeng, Y. Zhu, The crystal structure and chemical state of aluminum-doped hydroxyapatite by experimental and first principles calculation studies, Phys. Chem. Chem. Phys. 18 (2016) 21789–21796. https://doi.org/10.1039/C6CP03230C.
[22] N.P. Varma, A. Sinha, S.K. Gupta, J.K. Mahato, P. Chand, Enhanced defluoridation by nano-crystalline alum-doped hydroxyapatite and artificial intelligence (AI) modeling approach, Front. Environ. Sci. 12 (2024) 1363724. https://doi.org/10.3389/fenvs.2024.1363724.